Electronic Supplementary Material (ESI) for Journal of Materials Chemistry A.
This journal is © The Royal Society of Chemistry 2016

Supplementary materials

Structural origin of the superionic sodium conduction in $Na_2B_{10}H_{10}$ closo-borates and a potential way for conductivity enhancement for high performance solid electrolyte

1. Construction of the pseudo-cubic supercell from the monoclinic unitcell

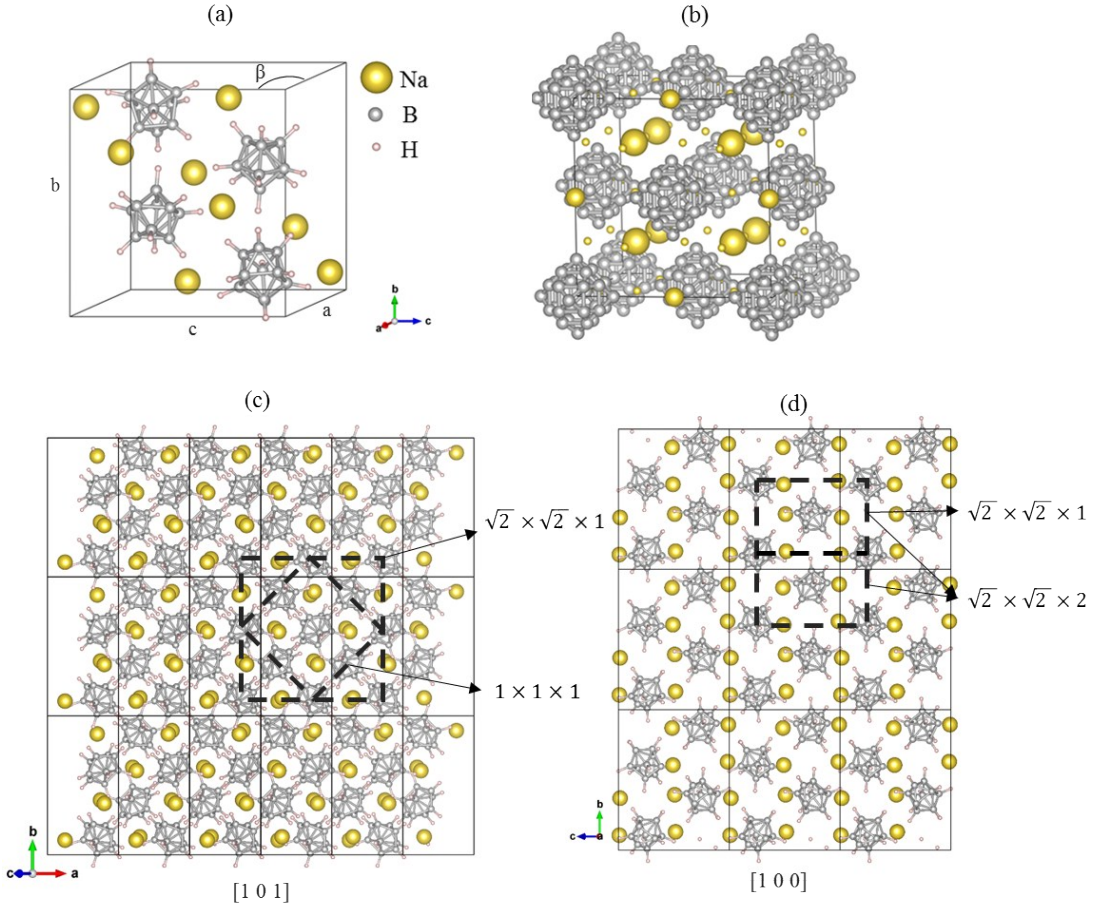

Fig. 1S. The primitive cells of the (a) monoclinic and (b) cubic phases. For the cubic phase, hydrogen atoms are omitted for clarity and the Na ion radii are manually tuned to be proportional to the experimentally derived occupancy. (c) and (d) show the projection of the monoclinic supercell along the [1 0 1] and the [1 1 0] direction. The construction of the cubic $1 \times 1 \times 1$, $\sqrt{2} \times \sqrt{2} \times 1$, and $\sqrt{2} \times \sqrt{2} \times 1$ supercells are illustrated.

The unit cells of the monoclinic phase and the cubic phase are shown in **Fig. 1S (a) and (b)**, respectively. We note that, despite the difference in orientation of the anionic groups and the high symmetry, their positions in the monoclinic phase are similar to those in the cubic phase if mapped accordingly. However, in the LT phase, the ordering of the anions leads to different symmetry making its primitive cell different from that of the cubic phase. Thus, to simulate the phase transition, we constructed a supercell which could reflect both the symmetry of LT and HT phase. The smallest supercell that is able to be mapped with the cubic phase and that can keep the ordered periodic structure of the monoclinic phase is the pseudo-cubic $\sqrt{2} \times \sqrt{2} \times 1$ supercell shown in **Fig. 1S, panels (b) and (c)**. The $1 \times 1 \times 1$ pseudo-cubic supercell is not actually periodic and thus is just used for illustration only.

2. NPT simulation details

The NPT simulations were carried out in a $\sqrt{2} \times \sqrt{2} \times 2$ pseudo-cubic supercell at 300K and 600K with a timestep of 0.5 fs. The pressure was kept constant at 1 atm using the variable cell approach.[1] We used the Parrinello-Rahman (NpT) scheme with a Langevin thermostat as implemented in VASP.[2, 3] For the current simulations, the pseudo-mass of lattice degree of freedom was set to be 1000 amu and friction coefficients of 1 ps^{-1} were used. All degrees of freedoms were allowed to change including the angles between lattice vectors. In order to eliminate Pulay stress, which could lead to poor sampling and numerical problems, we used a relatively large kinetic

cutoff of 550 eV (compared to the 350 eV for NVT simulations). The big simulation cell and large kinetic cutoff make the computations extremely expensive therefore we only simulated the systems for ~17 ps and stopped the simulation upon observing a phase change.

3. Labeling method

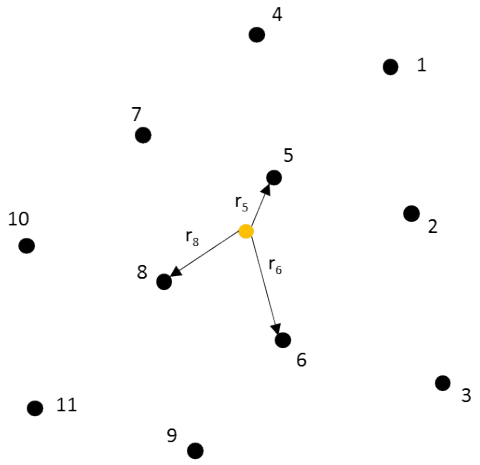

Fig. 2S Schematics of the labeling method. The orange dot indicates a representative Na ion and the black dots are the lattice sites as determined by crystallography.

The labeling of the Na ions is based on the shortest distance between the Na ions themselves and the static lattice sites. At each outputted simulation snapshot, we calculated the distance between each Na ion and every lattice site. We used this information to find the nearest site. As illustrated in **Fig. 2S**, a representative Na ion, marked as an orange dot, is labeled as 5 since site number 5 is the closest. The output of this labeling procedure is a time series data, which records the site index of each Na ion through the simulation. The data can be stored in a matrix $N_{Na} \times N_{steps}$, where

N_{Na} and N_{steps} are the total number of Na ions and the number of outputted simulation steps, respectively.

4. Lattice parameters obtained using different density functionals

LT phase	a(Å)	b(Å)	c(Å)	β(°)
Experiment [4]	6.6535	12.964	11.851	120.203
GGA-PBE	6.72990	13.13100	11.37743	120.2495
LDA	6.43795	12.54516	9.92420	120.2232
GGA-PBE-vdw-D2 [5]	6.31403	12.23220	9.96168	120.2024

5. Structural integrity

The mean squared displacements of B and H were extracted from the 2000K NVT simulation as introduced in the main text. The values do not increase after the first 2.5 ps as shown in **Fig. 3S (a)**, implying that neither B nor H are mobile in the current simulations. Therefore, no obvious lattice melting can be observed. In addition to that, we monitored the structural integrity of the $B_{10}H_{10}^{2-}$ cluster by tracking the B-H and B-B bond lengths for the entire duration of simulation. In order to detect any potential bond breaking, we monitored all bonds lengths starting from the initial structure. As shown in **Fig. 3S (b)**, we found that all the B-B and B-H bond lengths are distributed around their average values with no outliers detected suggesting that no bond breaking is observed for the B-B and B-H bonds.

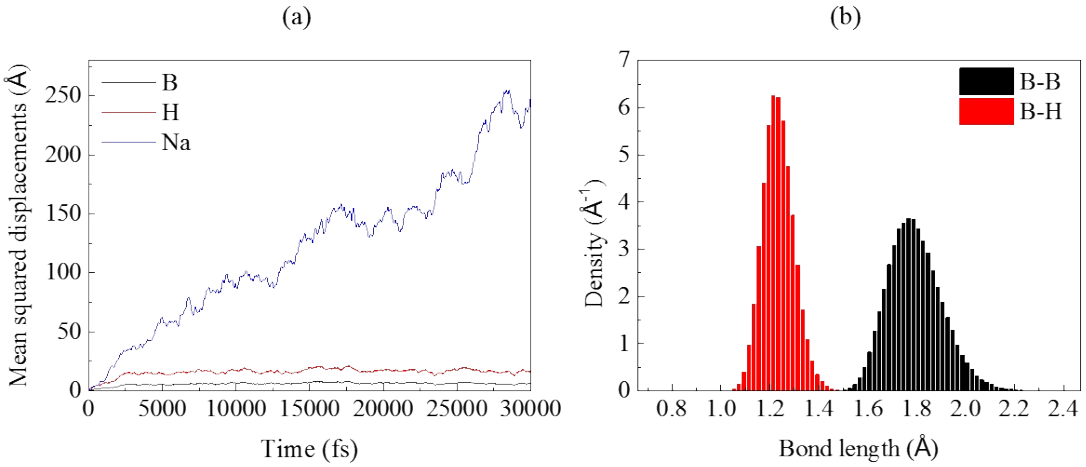

Fig. 3S (a) MSD of Na, B, H at 2000 K. (b) Density of B-H and B-B bond lengths at 2000 K. This histogram is calculated by binning the bond lengths data with a spacing of 0.01 ps and normalizing so that total area is unitary.

6. Nudged elastic band calculations for Na diffusion in LT and HT phases

The nudged elastic band (NEB) calculations are based on the climbing image algorithms developed by Henkelman *et al.*[6] For all the calculations shown in this work, 7 images were used and the force convergence criteria were set to 0.02 eV/Å. The energies of each image were calculated with the same settings as described in the Computational Methods section of the main article. For the LT phase, the $\sqrt{2} \times \sqrt{2} \times 1$ supercell as shown in **Fig. 9 (a)** of the main text was used as the starting structure. Then one Na^+ ion was removed from the supercell and the structure was further relaxed. This structure is used as the initial image. The construction of the final image is similar except that the Na^+ ion is removed from the neighboring Td site. The initial images for the NEB calculations are determined by linear interpolating the atomic positions in the starting and final images. For the HT phase, the calculation

method is the same as in the LT phase except that two anions are manually reoriented before further construction of the initial and final image. Since one Na^+ ion is removed from the supercell to create a vacancy, a uniform background charge is added to ensure the convergence of calculations. [7]

7. The periodic pseudo-density density and projection onto a sphere

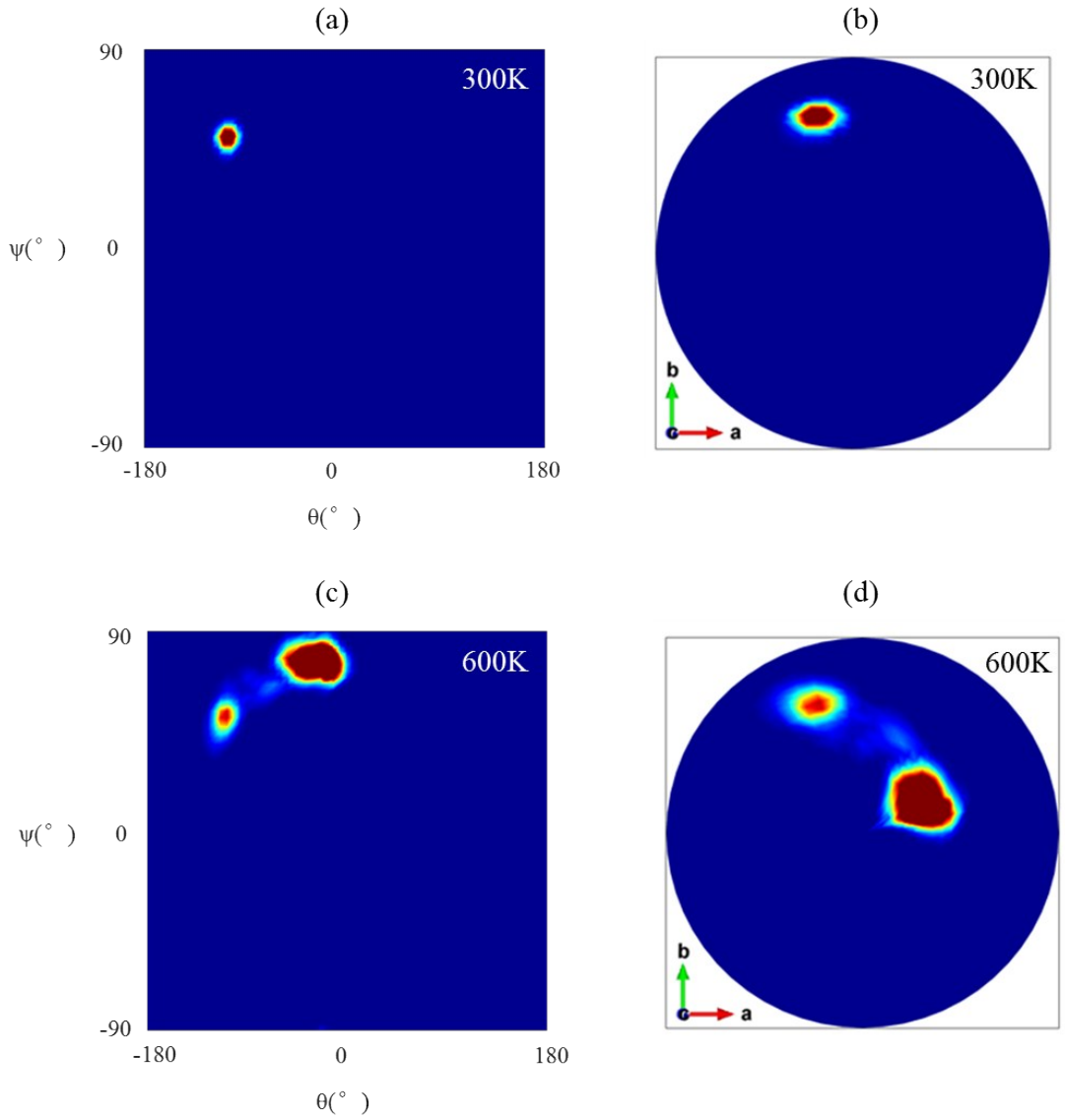

Fig. 4S Pseudo-angular densities of an anion at (a) 300K, (c) 600K and the corresponding projection onto a sphere (b) and (d).

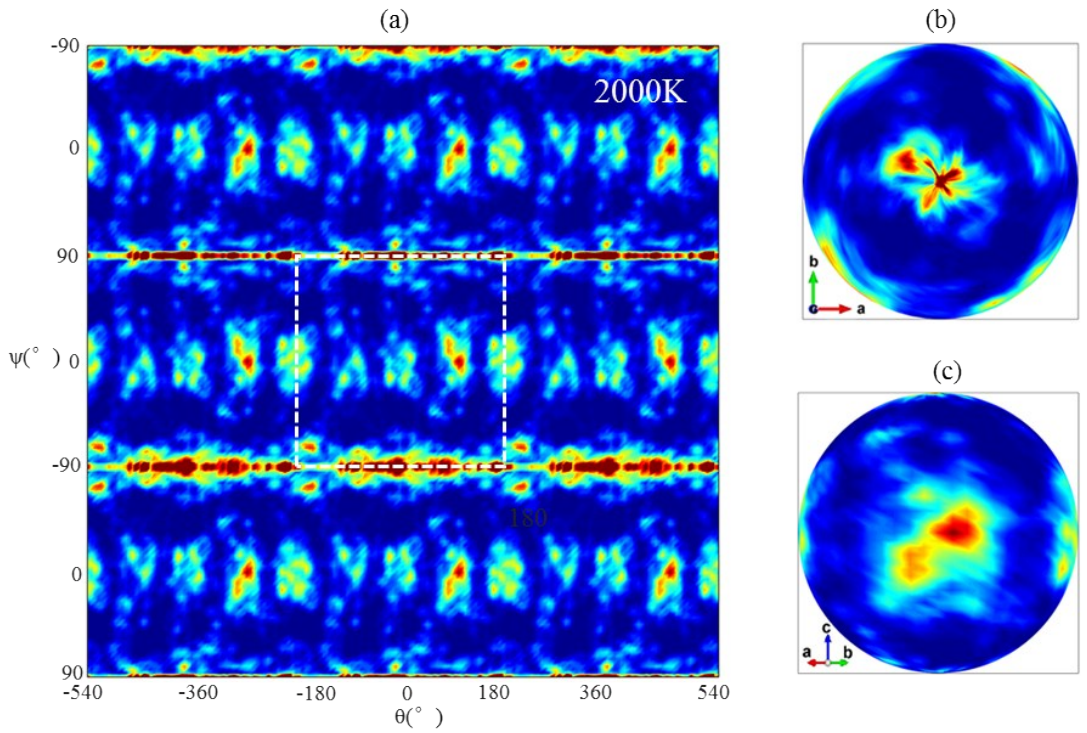

Fig. 5S (a) 3×3 periodic images of the angular densities of an anion at 2000K. (b) and (c) depict the densities projected onto a sphere and viewed from the [0 0 1] direction and the [1 1 0] direction, respectively.

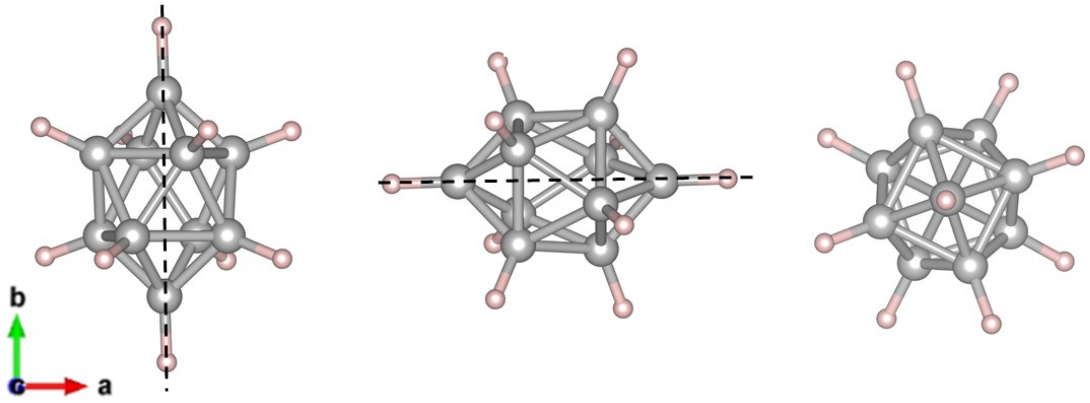

Fig. 6S Illustration of an anion align along the a, b, and, c axis.

Fig. 5S (a) shows the 3×3 periodic images of the angular densities of an anion at 2000K. The density is projected onto a sphere and the right panels show the results

viewed from the (b) [0 0 1] direction and the (c) [1 1 0] direction of the simulation cell. At 2000K, the orientations are highlighted with red boxes. Such patterns correspond to the anionic alignment along the a, b, and, c axis in the cubic unitcell as illustrated in **Fig. 6S**.

8. The Td-Td hopping and the Td-Oh (Oh-Td) hop

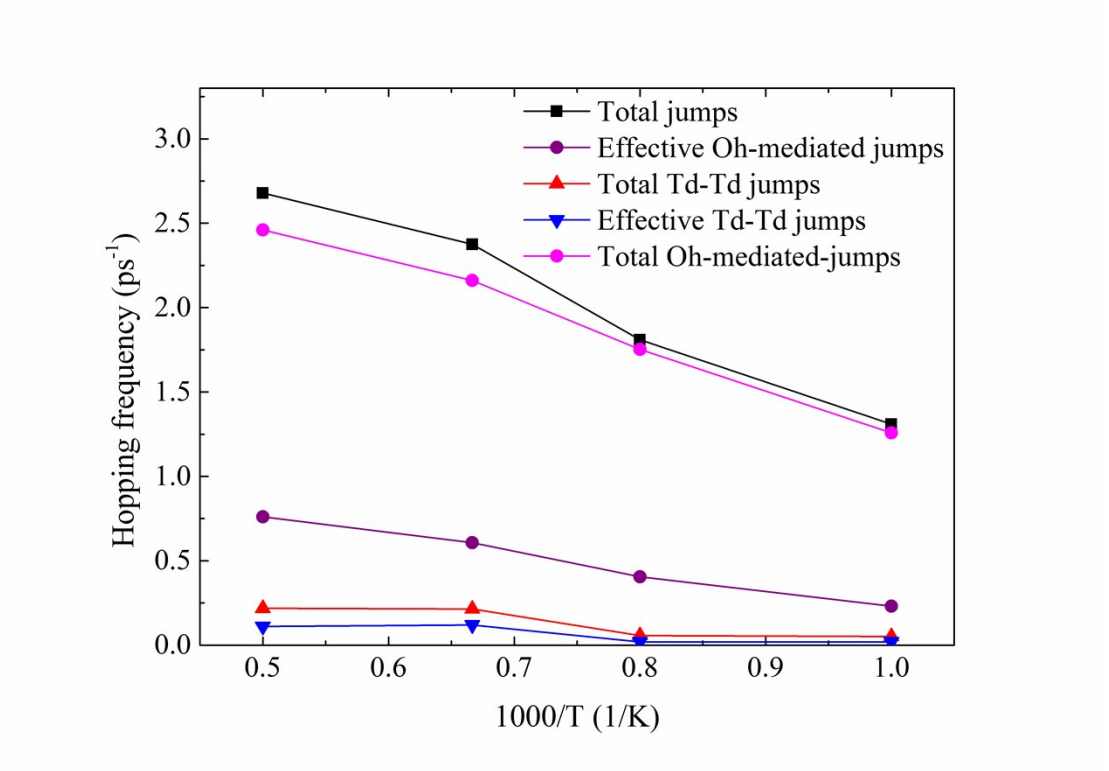

Fig. 7S the hopping frequencies of Td-Td jumps, Td-Oh/Oh-Td (Oh-mediated) jumps, effective Td-Td jumps, effective Oh-Td jumps and the total jumps.

Fig. 7S shows the average frequencies of different hopping events, which are computed as the total number of the given event divided by the simulation time. It is key to note that the jumps of Td-Td type are only a fraction of the others.

9. Na ionic conductivity

We obtained the corrected ionic conductivities using the modified Nernst-Einstein equation following the work of Lai and co-workers:[8 9]

$$\sigma = \Gamma^{-1}\frac{(ze)^2 Dc}{k_b T}$$

where σ is the ionic conductivity, Γ is the thermodynamic factor, ez is the charge of the charge carrier (Na^+ in this work), D is the diffusion coefficient, c is the concentration of the charge carrier, k_b is the Boltzmann constant, and T is the temperature. The thermodynamic factor Γ accounts for deviations from the dilute conditions and $\Gamma = 1$ represents such condition. We estimated the values of Γ by averaging the Na ions fluctuations in a 1/8 simulation box with $\Gamma = \langle N \rangle / {\sigma_N}^2$ where $\langle N \rangle$ and σ_N are the ensemble average of the particle numbers and its standard deviation.

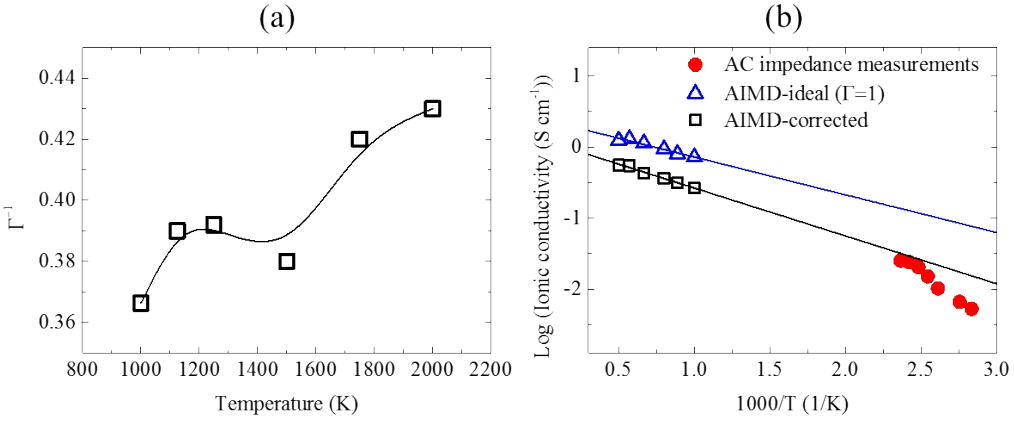

Fig. 8S. (a) Simulated inverse thermodynamic factors and (b) ionic conductivities derived from MD simulation. The AIMD-dilute data are calculated from the Nernst-Einstein equation and the AIMD-ideal corrected values are estimated by multiplying the thermodynamic factor by the non-corrected results. The experimental data are

adapted from T. J. Udovic *et al*. [4]

As shown in **Fig. 8S (a)**, the deviation of the thermodynamic factors from unity indicates that the Na ions behave non-ideally, i.e., the hopping of Na ions are not independent. The corrected Na ionic conductivities are shown in **Fig. 8S (b)** and it can be seen the extrapolated conductivities (0.022 S/cm at 383K) are comparable to those obtained from AC impedance ~0.01 S/cm at 383K). [4]

References

1. E. Hernández, The Journal of Chemical Physics, 2001, 115, 10282-10290.
2. M. Parrinello and A. Rahman, Physical Review Letters, 1980, 45, 1196.
3. M. Parrinello and A. Rahman, Journal of Applied physics, 1981, 52, 7182-7190.
4. T. J. Udovic, M. Matsuo, W. S. Tang, H. Wu, V. Stavila, A. V. Soloninin, R. V. Skoryunov, O. A. Babanova, A. V. Skripov and J. J. Rush, Advanced Materials, 2014, 26, 7622-7626.
5. J. Harl, L. Schimka and G. Kresse, Physical Review B, 2010, 81, 115126.
6. G. Henkelman, B. P. Uberuaga and H. Jónsson, The Journal of chemical physics, 2000, 113, 9901-9904.
7. C. Freysoldt, J. Neugebauer and C. G. Van de Walle, Physical review letters, 2009, 102, 016402.

8. Y. Wang, M. Klenk, K. Page and W. Lai, Chemistry of Materials, 2014, 26, 5613-5624.

9. M. Klenk and W. Lai, Physical Chemistry Chemical Physics, 2015, 17, 8758-8768.